

WPT System based on PSO Algorithm with Anti-Coupling Coefficient Change

Linna Yang^{1, a}, Zikai Li^{1, b} and Xin Ye^{1, c}

¹Xi'an Technological University, Xi'an 710021, China;

^a1039710293@qq.com, ^b363171049@qq.com, ^cye17829094644@163.com

Abstract

To address the issue of significant fluctuations in system output power caused by offset between the transmitting and receiving coils during wireless charging of WPT systems, a WPT system with anti coupling coefficient variation characteristics is studied. This article first proposes a suitable hybrid compensation network. Secondly, design a coupling mechanism with anti offset characteristics, and based on this, optimize the circuit parameters using the PSO algorithm to ensure that the system can output constant power during offset. Finally, a 180W prototype was built, and the experimental results showed that the variation range of the system coupling coefficient was between 0.4 and 0.62, and the output power fluctuation of the coefficient was not more than 12%.

Keywords

Particle Swarm Optimization; Parameter optimization; Wireless charging; Resistance to coupling coefficient variation.

1. Introduction

Wireless Power Transfer (WPT) technology is a non-contact power transmission technology that utilizes electromagnetic fields. It has the advantages of safety, reliability, and environmental friendliness, and has been widely used in various fields. However, in practical applications, it is impossible to fully align the coupling mechanisms^[1], resulting in energy loss. Generally speaking, the coupling coefficient between the transmitting coil and the receiving coil decreases with the increase of offset distance. When the coupling coefficient is too small, the power transmission ability weakens, and the output power fluctuation increases, affecting the efficiency and stability of the system. Therefore, studying the anti offset characteristics of WPT systems ultimately boils down to studying the changes in the anti coupling coefficient of the system.

In practical applications, the relative position deviation between coupling coils can affect the stability of the system. In order to solve this problem, many scholars both domestically and internationally have explored control strategies, compensation networks, coupling mechanisms, and parameter optimization^[2]. In terms of control strategies, reference^[3] introduces a Buck Boost converter to achieve more precise energy regulation, proposes a mode switching strategy, reduces energy loss, and improves transmission efficiency.

In terms of coupling structure, reference^[4] proposes a novel LCT-TC coupling model, which exhibits astonishing performance in experiments due to its unique structure of reverse series connection between the primary coil and the third coil. The experimental results show that the model has an offset percentage of up to 40% and an output efficiency of no less than 92%.

This paper addresses the issues of decreased mutual inductance coefficient, low power utilization of system inverters, and output power fluctuations caused by secondary coil offset^[5]. A WPT system based on PSO algorithm is designed, with the research goal of resisting coupling coefficient changes in radio energy transmission. By utilizing the fundamental and third

harmonic components of the square wave voltage output from the full bridge inverter, a suitable compensation network and coupling mechanism are constructed to improve the offset fault tolerance of the WPT system.

2. WPT system design

The coupling coefficient and efficiency of a system during offset are important indicators to measure its anti offset performance. In order to analyze the performance of the system, it is necessary to first obtain the transmission efficiency and power of the system based on the resonance compensation topology. As the mutual inductance coupling model is closely related to the topology structure, it is also necessary to analyze the impact of different resonance compensation topologies on the mutual inductance coupling model, in order to determine the optimal resonance compensation network.

The coupling coefficient k of SS compensation network and LCC-S compensation network system, as well as the influence of load R on output power P , can be offset by reasonably adding parameters to propose a hybrid compensation network. The WPT system structure is shown in Figure 1. On the left is a full bridge inverter, which converts DC voltage and current into AC voltage and current. The output AC square wave voltage can be decomposed into Fourier series of fundamental harmonics and odd harmonics. Is the total harmonic current of the n th input and the total harmonic current of the n th output. On the right side, a rectifier and a filtering capacitor are used to rectify and output DC voltage to supply power to the load.

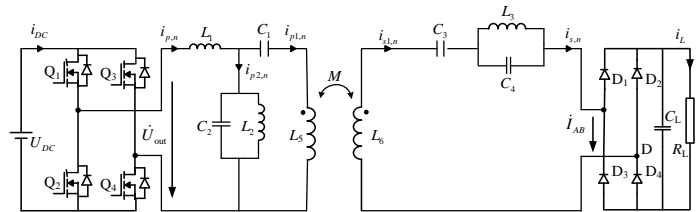


Figure 1 Overall Structure of a Hybrid Topology WPT System

According to the topology circuit and dual frequency tuning method, write the KVL and KCL equations of the circuit as follows,

$$\begin{bmatrix} U_{in,n} \\ 0 \\ 0 \end{bmatrix} = \begin{bmatrix} Z_{11} & Z_{12} & Z_{13} & Z_{14} \\ Z_{21} & Z_{22} & Z_{23} & Z_{24} \\ Z_{31} & Z_{32} & Z_{33} & Z_{34} \end{bmatrix} \begin{bmatrix} i_{p,n} \\ i_{p1,n} \\ i_{p2,n} \\ i_{s1,n} \end{bmatrix}, n = 1, 3 \quad (1)$$

Among them:

$$\begin{cases} Z_{11} = j\omega_n L_1 \\ Z_{12} = Z_{14} = Z_{21} = Z_{31} = Z_{33} = 0 \\ Z_{13} = \frac{j\omega_n L_2}{1 - \omega_n^2 L_2 C_2} \\ Z_{22} = j\omega_n L_5 + \frac{1}{j\omega_n C_1} \\ Z_{23} = -\frac{j\omega_n L_2}{1 - \omega_n^2 L_2 C_2} \\ Z_{24} = Z_{32} = -j\omega_n M \\ Z_{34} = j\omega_n L_6 + \frac{1}{j\omega_n C_3} + \frac{j\omega_n L_3}{1 - \omega_n^2 L_3 C_4} + R_e \end{cases} \quad (2)$$

In order to achieve dual frequency power transmission, the parameter design of each component in a hybrid topology circuit should meet certain constraints. When only considering

the fundamental component of the square wave voltage, the parameters should meet equation (3).

$$\begin{cases} \omega_1 L_2 = \frac{1}{\omega_1 C_2} \\ \omega_1 (L_1 + L_5) = \frac{1}{\omega_1 C_1} \\ \omega_1 L_{e1} = \frac{1}{\omega_1 C_{e1}} \end{cases} \quad (3)$$

Among ω_1 represents the angular frequency of f_1 , while L_{e1} and C_{e1} represent the equivalent inductance and capacitance of the secondary compensation network when only considering the fundamental component. The sizes of L_{e1} and C_{e1} are shown in equation (4).

$$\begin{cases} j\omega_1 L_6 + \frac{1}{j\omega_1 C_3} = \frac{1}{j\omega_1 C_{e1}} \\ \frac{j\omega_1 L_3}{1 - \omega_1^2 L_3 C_4} = j\omega_1 L_{e1} \end{cases} \quad (4)$$

When only considering the third harmonic component, the parameter should satisfy equation (5), where ω_3 is the angular frequency of f_3 .

$$\begin{cases} \omega_3 L_1 = \frac{1}{\omega_3 C_x} \\ \omega_3 L_{e2} = \frac{1}{\omega_3 C_{e2}} \\ \omega_3 L_p = \frac{1}{\omega_3 C_x} \end{cases} \quad (5)$$

Among them, L_p and C_x represent the equivalent inductance and capacitance L_{e2} of the primary compensation network when only considering the third harmonic component, and C_{e2} represent the equivalent inductance and capacitance of the secondary compensation network when only considering the third harmonic component. The sizes of L_p , C_x , L_{e2} , and C_{e2} are shown in equation (6).

$$\begin{cases} \frac{j\omega_3 L_2}{1 - \omega_3^2 L_2 C_2} = \frac{1}{j\omega_3 C_x} \\ j\omega_3 L_5 + \frac{1}{j\omega_3 C_1} = j\omega_3 L_p \\ j\omega_3 L_6 + \frac{1}{j\omega_3 C_3} = j\omega_3 L_{e2} \\ \frac{j\omega_3 L_3}{1 - \omega_3^2 L_3 C_4} = \frac{1}{j\omega_3 C_{e2}} \end{cases} \quad (6)$$

Equation (7) represents the current at the fundamental frequency and equation (8) represents the current at the third harmonic frequency.

$$\begin{cases} i_{p1,1} = \frac{U_{in,1}}{\omega_1^2 M^2} R_e \\ i_{s1,1} = \frac{jU_{in,1}}{\omega_1 M} \end{cases} \quad (7)$$

$$\begin{cases} i_{p1,3} = \frac{U_{in,3}}{j\omega_3 L_1} \\ i_{s1,3} = \frac{MU_{in,3}}{L_1 R_e} \end{cases} \quad (8)$$

The effective voltage values of the fundamental and third harmonics can be described as:

$$U_{in,1} = U_{in}(\omega = \omega_1) = \frac{2\sqrt{2}U_{dc}}{\pi} \quad (9)$$

$$U_{in,3} = U_{in}(\omega = \omega_3) = \frac{2\sqrt{2}U_{dc}}{3\pi} \quad (10)$$

The output power of the system can be obtained as:

$$P_{out} = \sum_{n=1,3} I_{s,n}^2 R_e = P_1 + P_2 = \frac{4U_{DC}^2}{\pi^2} \left(\frac{R_e}{\omega_1^2 M^2} + \frac{M^2}{9L_1^2 R_e} \right) \quad (11)$$

3. Coupling mechanism

In order to improve the transmission distance between coupling mechanisms, an asymmetric coupling structure with a transmitting (primary) coil shape larger than the receiving (secondary) coil is designed to solve the problem of the transmitting coil having no transmission capacity when the receiving coil offset is large. The transmission characteristics of the coil are related to the number of turns and the size of the inner and outer sides. Due to the structural characteristics of the asymmetric coupling mechanism, using the control single variable method is more complex. A parameter optimization method is proposed, and the ANSYS Maxwell finite element simulation software is used for parameter design to obtain the optimal solution of the parameters and obtain the optimal coil structure under this combination. Simulate the curves between the coupling coefficients and offsets corresponding to different models in Maxwell, as shown in Figure 2.

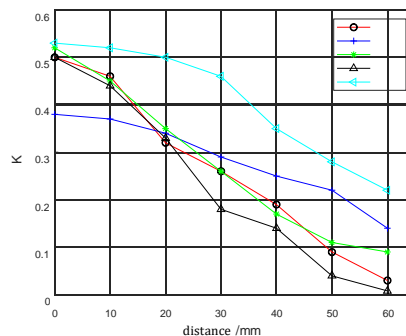


Figure 2 Curve Chart of Coupling Coefficients of Different Groups Changing with Offset

According to the coupling coefficient curve in Figure 2, when the inner diameter and side length of the primary and secondary coils are equal, and the outer diameter and side length of the primary coil are slightly larger than the secondary coil, the coupling mechanism has the highest coupling coefficient and the strongest transmission capacity when fully aligned. Moreover, as the offset increases, the coupling coefficient coefficient changes more smoothly, and the anti offset characteristics of the coupling mechanism will be improved. At the same time, the size and number of turns of the coupling mechanism are also important factors affecting its

transmission capacity. The larger the size and number of turns, the stronger the transmission capacity of the coupling mechanism, but this will also increase its volume and cost. Use Maxwell simulation software to establish a 3D coupled mechanism model, as shown in Figure 3.

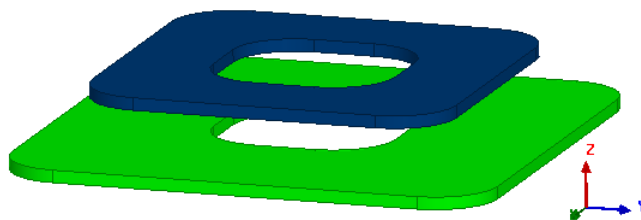


Figure 3 3D coupled mechanism model

When the coupling mechanism has no offset, the magnetic induction intensity is the highest, and the transmission capacity is the strongest at this time. In different directions and offsets, the magnetic field lines passing vertically through the coupling mechanism are inversely proportional to the offset. The magnetic field lines between the coils gradually decrease with the increase of the offset, that is, the main magnetic flux decreases, while the emitted magnetic field lines around the coils increase, that is, the leakage magnetic flux increases. Therefore, the larger the offset, the smaller the main magnetic flux, the greater the leakage magnetic flux, and the weaker the transmission capacity.

4. Parameter Optimization Design Based on PSO Algorithm

The traditional system parameter determination mainly relies on experience, and the determination of parameters lacks theoretical basis and has randomness. In order to ensure the high transmission efficiency of the system, this paper uses particle swarm optimization (PSO) to optimize the circuit parameters of WPT system. This algorithm was first proposed by James Kennedy in 1995, and its idea originated from Craig W. Reynolds' Bodies model. PSO is suitable for solving nonlinear problems, with advantages such as low cost and being unaffected by problem dimensions.

The specific working principle of the algorithm is as follows: PSO will randomly assign initial values to each particle at the beginning. During the optimization process, the particle position is constantly updated, and the fitness function is used to judge the current solution and gradually obtain the global optimal solution, which has the advantages of simplicity, efficiency, fast convergence and few parameters.

To clarify the optimization objectives, they can be divided into the following steps for discussion:

Step 1: When the load is constant and the offset between the receiving coil and the transmitting coil is different, the output power fluctuation of the system is minimized;

Step 2: When the offset is constant and the system load changes, the output power fluctuation of the system is minimized;

Step 3: Within the range of coil offset and load variation, the output power fluctuation of the system is minimized.

After the above analysis, the problem of resisting load disturbance and offset disturbance is discussed step by step. When the load is constant, the output power changes with the coil offset. Further deformation of the system's output power equation (4.5), resulting in

$$A = \frac{U_{DC}^2 L_5 L_6}{18 R L_1^2} \quad (12)$$

$$B = \frac{32U_{DC}^2 R}{\pi^4 \omega_1^2 L_5 L_6} \tag{13}$$

Then, the output power of the system can be expressed as, as shown in equation (4.10).

$$P_{out} = Ak^2 + B \frac{1}{k^2} \tag{14}$$

It can be seen from equation (14) that when A and B are regarded as constant coefficients by mathematical analysis, this equation represents the relationship between output power and coupling coefficient. When A and B obtain appropriate values, this expression can be regarded as a tick function to obtain the ideal relationship between output power and coupling coefficient, as shown in Figure 4 below.

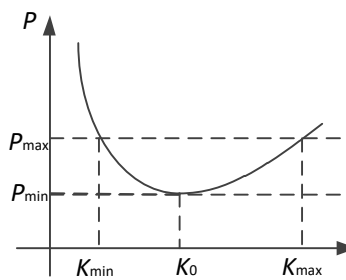


Figure 4 Schematic diagram of P-K curve relationship

From Figure 4, it can be seen that when A and B obtain appropriate parameters, the output power first decreases and then increases with the increase of the coupling coefficient. This trend change can cause the system output power to fluctuate within the allowable deviation range, and the range of the system coupling coefficient reaches the maximum, that is, the offset range between the receiving coil and the transmitting coil of the coupling mechanism reaches the maximum, and the system has the best anti offset performance.

Due to the existence of this nonlinear relationship, there may also be discontinuities between data points, which will pose certain challenges to the performance of the system. To overcome these issues, more refined modeling and parameter selection methods are needed to better understand and optimize the performance of the system.

To solve this problem, the optimization problem is transformed into finding the minimum value of output power fluctuation within the coupling coefficient range and load range, and the objective function is shown in equation (15).

$$\min Y = f = (f_1, f_2, f_3 \dots f_n) \tag{15}$$

$$f_n = \max Z = \left| \frac{P_n - P}{P} \right| \tag{16}$$

In equation (16), P_n represents the output power of each system at different offsets and loads. Based on the model established above regarding output power, after comprehensive consideration, the constraint conditions are shown in equation (17).

$$\begin{cases} k_{\min} < k < k_{\max} \\ L_{\min} < L_1 < L_{\max} \\ R_{\min} < R < R_{\max} \end{cases} \tag{17}$$

The determination of the solution space has a significant impact on the solution results. If the solution space is too small, it may not cover the optimal solution; When it is too large, it will be

difficult to search for the optimal solution. The parameters in equation (17) are all unique physical quantities in the physical circuit. According to practice, if they are all positive numbers, the minimum values are all greater than 0.

In order to find the best parameter value, this paper uses MATLAB software to analyze and optimize each parameter, and determines the best parameter value by comparing the fitness values under different parameter combinations. Figure 5 shows the change curve of fitness value with the number of iterations, and shows the optimal error value of output power fluctuation after optimization of algorithm parameters.

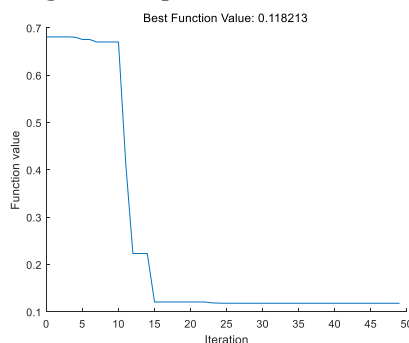


Figure 5 fitness Change Curve

Figure 5 shows the change of fitness value with the number of iterations in the PSO algorithm. The fitness value is a measure of the fluctuation of the system output power. The smaller the fitness value is, the smaller the fluctuation of the system output power is, the more stable the system is.

When the number of iterations reaches a certain value, the fitness value is basically unchanged. At this time, the maximum fluctuation of the system output power is 0.118213, indicating that the WPT system has good stable output characteristics, and the results reach the expected goal. The parameters in the compensation circuit are optimized using the method presented in this article, and the values of each parameter are shown in Table 1.

Table 1 Table of optimized parameter values

parameter	Value
L_1	21.6uH
K	0.41-0.62
R	2Ω-4Ω
Optimized output power P fluctuation ratio	±12%

5. Experimental verification

In order to verify the anti offset performance of the WPT system designed in this article, an experimental platform was constructed according to the optimized component parameter values shown in Table 1, as shown in Figure 6. However, in practical applications, the accuracy of component parameters is limited by manufacturing processes and environmental factors, resulting in a certain deviation between the actual measured parameter values and the theoretical analysis parameter values. These factors will all affect the experimental results of the wireless charging system, making it inconsistent with the simulation results in the previous section.



Figure 6 WPT System Experimental Platform

The equivalent load resistance value for system charging is selected from $2\ \Omega$ to $4\ \Omega$, and the relative position of the receiving coil and the transmitting coil is changed. The voltage and current at the output and load ends of the inverter are collected, and the changes in system output power under different loads and offsets are analyzed and calculated.

Multiple experiments were conducted with a system load of $2\ \Omega$ - $4\ \Omega$ and a coupling coefficient range of 0.41-0.62. The experimental results are shown in Figure 7.

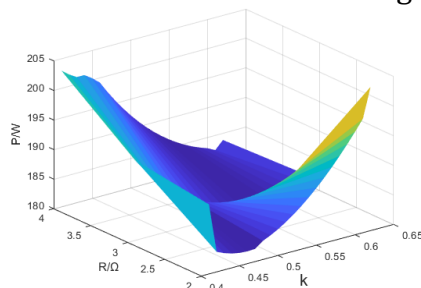


Figure 7 Curve of Output Power Changing with Coupling Coefficient and Load

According to the output power variation curve in Figure 7, when the load range is $2\ \Omega$ - $4\ \Omega$ and the coupling coefficient range is 0.41-0.62, the output power of the system is between 180.2W-201.8W, with a fluctuation of no more than 12%. As the coupling coefficient decreases, the output power first decreases and then increases. When k is large, the output power decreases with the increase of R . At this time, the power is mainly provided by the third harmonic. When k is small, the output power increases with the increase of R , mainly provided by the fundamental wave. The correctness and reliability of the theoretical analysis have been proven through the analysis of experimental results.

6. Conclusion

This article proposes a WPT system design method based on the PSO algorithm, which does not require complex control strategies. It optimizes the parameters of the mixed topology structure of the system, accelerates the calculation speed, and has accurate calculation accuracy. The output power of the system under the optimal parameters obtained by this method is relatively stable. In the article, the topology of SS and LCC-S is analyzed first, and the parameters of the asymmetric coupling mechanism are optimized. Secondly, in order to achieve better resistance to coupling coefficient changes in the system, the PSO algorithm is proposed to optimize the system circuit parameters. Finally, a 180W experimental prototype was built, and the experimental results showed that the output power fluctuation of the system was not more than 12% when the coupling coefficient range was 0.4-0.62.

References

- [1] R.K. Mai, Y. Li: Radio Energy Transmission Technology and Its Research Progress in Rail Transit Crane Design Manual [J] Journal of Southwest Jiaotong University,2016,51(3):446-459.

- [2] Huang L, Hu A P, Swain A K, et al. Z-impedance Compensation for Wireless Power Transfer Based on Electric Field[J]. IEEE Transactions on Power Electronics, 2016, 31(11): 7556-7563.
- [3] Budhia M Covic GA Boys JT. Design and optimization of circular magnetic structures for lumped inductive power transfer systems [J]. IEEE Transactions on Power Electronics, 2011 26 (11):3096-3108.
- [4] Budhia M, Boys J T, Covic G A, et al. Development of a Single-Sided Flux Magnetic Coupler for Electric Vehicle IPT Charging Systems[J]. IEEE Transactions on Industrial Electronics, 2013, 60(1): 318-328.
- [5] Chen Y, Mai R, Zhang Y, et al. Improving misalignment tolerance for IPT system using a third-coil[J]. IEEE Transactions on Power Electronics, 2019, 34(4): 3009-3013.